



UVA-induced metabolic changes in non-malignant skin cells and the potential role of pyruvate as antioxidant

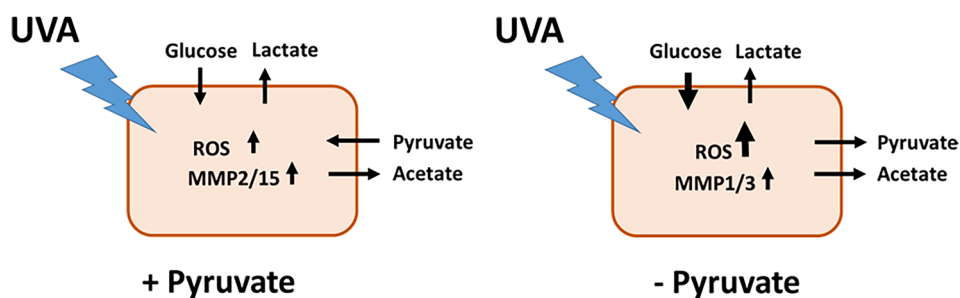
I. Ivanova¹ · C. Bogner² · W. Gronwald² · M. Kreutz³ · B. Kurz¹ · T. Maisch¹ · Y. Kamenisch¹ · M. Berneburg¹

Received: 20 January 2023 / Accepted: 4 April 2023
© The Author(s) 2023

Abstract

The exposure to UVA (320–400 nm) irradiation is a major threat to human skin concerning photoaging and carcinogenesis. It has been shown that UVA irradiation can induce reactive oxygen species (ROS) and DNA mutations, such as 8-hydroxydeoxyguanosine. Furthermore, UVA induces the expression of photoaging-associated matrix metalloproteases (MMPs), especially of matrix metalloprotease 1 (MMP 1) and matrix metalloprotease 3 (MMP 3). In addition to this, it was recently shown that UVA-induced ROS also increase glucose metabolism of melanoma cells, however, the influence of UVA on the glucose metabolism of non-malignant cells of the human skin has, so far, not been investigated in detail. Here, we investigated the UVA-induced changes in glucose metabolism and the functional relevance of these changes in primary fibroblasts—normal non-malignant cells of the skin. These cells showed an UVA-induced enhanced glucose consumption and lactate production and changes in pyruvate production. As it has been proposed that pyruvate could have antioxidant properties we tested the functional relevance of pyruvate as protective agent against UVA-induced ROS. Our initial experiments support earlier publications, demonstrating that pyruvate treated with H₂O₂ is non-enzymatically transformed to acetate. Furthermore, we show that this decarboxylation of pyruvate to acetate also occurs upon UVA irradiation. In addition to this, we could show that in fibroblasts pyruvate has antioxidant properties as enhanced levels of pyruvate protect cells from UVA-induced ROS and partially from a DNA mutation by the modified base 8-hydroxydeoxyguanosine. Furthermore, we describe for the first time, that the interaction of UVA with pyruvate is relevant for the regulation of photoaging-associated MMP 1 and MMP 3 expression.

Graphical abstract



Keywords Non-malignant dermal cells · Glucose metabolism · Ultraviolet (UV) radiation · Reactive oxygen species · MMP · Pyruvate

Abbreviations

8-OHdG	8-Hydroxydeoxyguanosine
ATP	Adenosine triphosphate
CPMG	Carr–Purcell–Meiboom–Gill
D2O	Deuterium oxide
Ex/Em	Excitation/emission

Kamenisch and Berneburg have contributed equally to this work.

Extended author information available on the last page of the article

FA	Formic acid
MED	Minimal erythema dose
MMP	Matrix metalloprotease
NMR	Nuclear magnetic resonance
pyr	Pyruvate
ROS	Reactive oxygen species
TSP	Trimethylsilylpropanoic acid
UV	Ultraviolet

1 Introduction

From the UV-radiation reaching the Earth's surface, the major part consist of UVA (320–400 nm, further subdivided to UVA2 (320–340 nm) and UVA1 (340–400 nm)) radiation (95%), with the rest being UVB [1, 2]. In comparison to UVB, UVA is not blocked by the most types of window glass, resulting in higher daily exposure to this type of radiation in particular [3, 4]. The damaging effect of UVA to the skin is well known with UVA-induced reactive oxygen species (ROS) as an important mutagen [5, 6]. These ROS can cause oxidative damage to proteins or DNA. One prominent type of ROS-induced DNA damage is an oxidized guanosine, the 8-hydroxydeoxyguanosine, which can block transcription [7] and can give rise to error prone replication (predominantly GC to TA transversions) [8].

A sufficient energy supply is a prerequisite for the cell to be able to adequately react to UVA-induced cellular stress and damage, and carbohydrates (amongst others glucose) are the main source of energy for human cells [9]. One very important part of glucose metabolism is glycolysis, which converts glucose in several steps to pyruvate and generates adenosine triphosphate (ATP) from ADP and phosphate. Consecutively pyruvate can be metabolized to lactate or, when sufficient oxygen is present, can be completely oxidized to CO₂ in the mitochondria, which constitutes the major source of ATP. Many non-proliferating cells prefer the latter pathway to maximize ATP output (reviewed in van der Heiden et al. [10]). However, there are some subsets of malignant and non-malignant cells that prefer to metabolize glucose to lactate even in the presence of oxygen in a process known as aerobic glycolysis [11]. This enhanced consumption of glucose, even in the presence of oxygen, was first described by Otto Warburg and termed Warburg effect [12].

In their 2016 publication, Kamenisch et al. showed a connection between UVA and increased glucose and lactate metabolism in human primary melanoma cells [13]. However, the important question whether UV radiation can change the glucose metabolism in non-malignant dermal cells has not been comprehensively investigated yet. Recent publications point to metabolic changes in the skin upon

UVB irradiation [14, 15] but the current information on the UVA-induced changes in glucose metabolism in dermal cells has been collected mainly from genomic analysis [16] and still remains incomplete, especially when cell treatment with sub-erythema doses of UVA is concerned.

As glycolysis is crucial part of cell metabolism, and shows distinct UVA-regulation in malignant skin cells, it is important to take into consideration that pyruvate, an intermediate product of glycolysis, is a common additive in some cell culture media. Pyruvate is known to possess antioxidant properties [17–19] and to have protective effects against UVB damage [20]. However, its influence on the UVA response in skin and non-malignant skin cells is still unclear.

Here we show that UVA irradiation enhances glucose consumption and lactate production in human non-malignant fibroblasts indicating a uniform response to UVA treatment which is not restricted to malignant cells. Furthermore, the observed pattern of pyruvate regulation after UVA irradiation points to a possible antioxidant role of pyruvate in irradiated skin. We also confirm that pyruvate can be non-enzymatically converted to acetate in the presence of H₂O₂ or UVA irradiation. We show that pyruvate decreases UVA-induced ROS and can alleviate the 8-hydroxydeoxyguanosine induction.

Although it has been separately investigated if UVA [13, 21] or pyruvate [22] can influence the expression of MMPs, we were able to show that pyruvate can reduce the effects of UVA on the expression of MMP1 and MMP3, which are associated with photoaging.

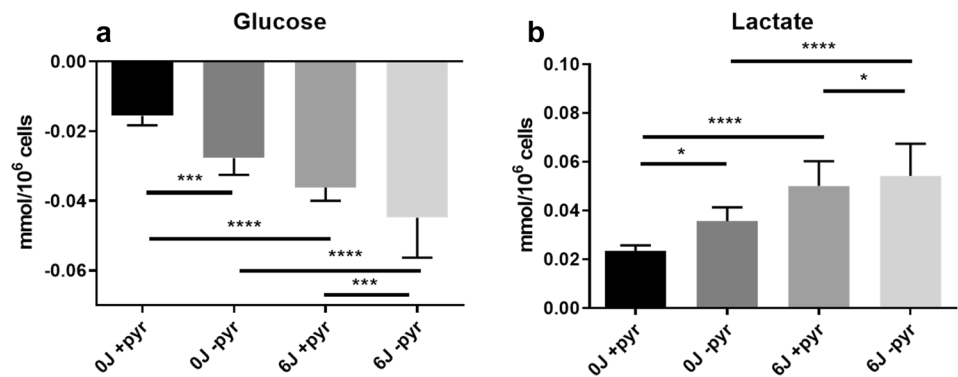
2 Results

2.1 UVA and pyruvate modulate glucose consumption and lactate production in primary human fibroblasts

Primary human fibroblasts were irradiated with UVA (6 J/cm²) three times per day for 4 consecutive days in medium with (1 mM) or without pyruvate (Irradiation Protocol depicted in Supplementary Figure S. 1a). The specifications of the used UVA-lamp are shown in Supplementary Figure S. 2. The irradiation resulted in proliferation retardation in both experiments with and without pyruvate. However, there were no changes in cell viability and the number of cells did not fall under the initially seeded amount (see Supplementary Figure S. 3).

After the irradiation, the cell supernatant was collected for metabolic analysis. Metabolic analysis was performed by ¹D ¹H CPMG-NMR. Glucose consumption and lactate production were measured in absence or presence of UVA

Fig. 1 UVA-irradiation increases glucose consumption (a) and lactate production (b) in human fibroblasts after 4 days repetitive irradiation with $3 \times 6 \text{ J/cm}^2$ UVA per day. (Statistical analysis: Two-way ANOVA with Bonferroni's multiple comparisons test, For significances: (*) $P < 0.05$; (***) $P < 0.0005$; (****) $P < 0.0001$). *J* Joule, *pyr* pyruvate

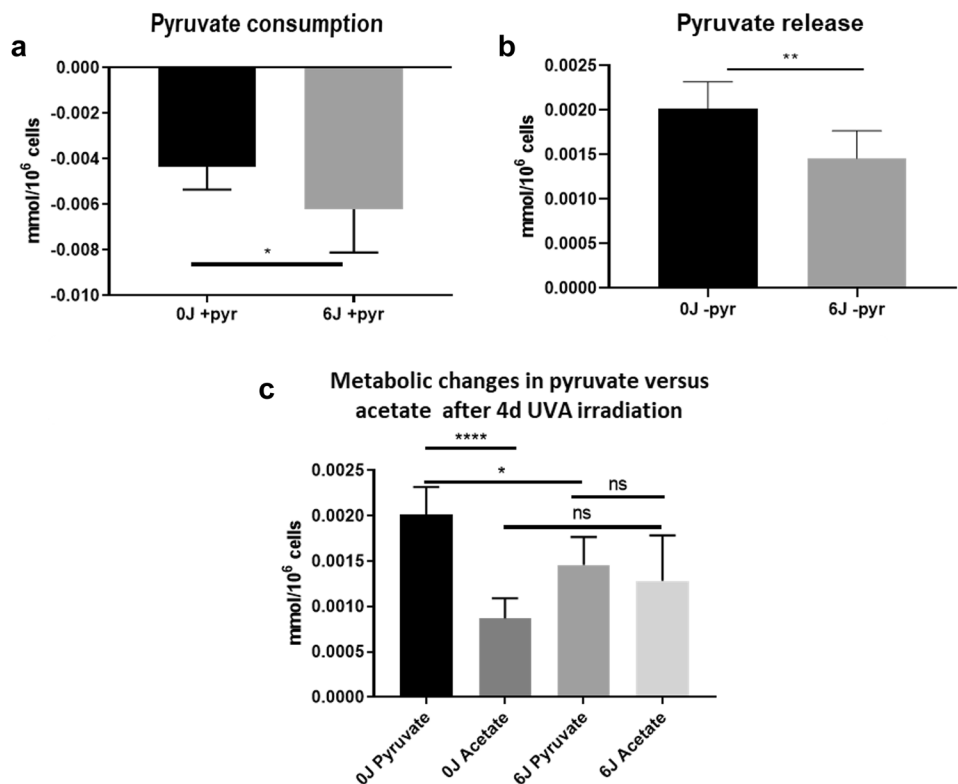


and pyruvate exposure. When observing cells cultured in standard medium (1 mM pyruvate), fibroblasts showed a significant increase in glucose consumption (Fig. 1a) and lactate production (Fig. 1b) after UVA irradiation compared to non-irradiated controls. This increase in glucose metabolism was enhanced by the absence of pyruvate in the cell culture medium. Glucose consumption was significantly increased in both irradiated and un-irradiated samples without pyruvate, compared to their corresponding 1 mM pyruvate counterparts. There was also an enhancement of lactate secretion into the medium by both irradiated and un-irradiated cells cultured in the absence of pyruvate, compared to their corresponding 1 mM pyruvate counterparts (see Fig. 1).

2.2 UVA and pyruvate regulate cellular metabolism beyond glucose and lactate

Fibroblasts cultivated in medium with and without pyruvate medium were treated with and without UVA irradiation (see Supplementary Figure S 1a) with subsequent measurement of the pyruvate concentration. When 1 mM pyruvate is added to the medium UVA treated cells consume more pyruvate compared to untreated control (Fig. 2a). When cells are cultivated in medium without pyruvate the cells produce and secrete pyruvate (Fig. 2b) but the concentration of secreted pyruvate decreases upon UVA irradiation indicating that a part of the pyruvate production is consumed by ROS dependent conversion to acetate. Acetate, which can be a product of ROS-induced

Fig. 2 Human fibroblasts cultured in medium containing pyruvate have increased pyruvate consumption after UVA-irradiation, compared to un-irradiated controls (a). Cells grown in the absence of pyruvate release pyruvate into the medium. After UVA irradiation, pyruvate release decreases, compared to un-irradiated controls (b). In samples cultured without pyruvate, the amount of acetate present in the medium increases after irradiation (c). (Statistical analysis: Student t-test; Two-way ANOVA with Bonferroni's multiple comparisons test, For significances: (ns) $P > 0.05$; (*) $P < 0.05$; (**) $P < 0.005$; (****) $P < 0.0001$) *J* Joule, *pyr* pyruvate, *ns* not significant



pyruvate decomposition, is released in the cell culture medium to a higher degree after UVA treatment (Fig. 2c). This, albeit non-significant, increase in secretion of acetate also correlates with a decrease in the total amount of released pyruvate (Fig. 2c).

After detecting changes in glucose, lactate and pyruvate metabolism, it was of interest to see whether other key metabolites would change with UVA treatment or pyruvate depletion. UVA irradiation resulted in increase in glutamine consumption, glutamate release, and cystine consumption in the cell supernatant (Supplementary Figures S. 4a, b and c respectively). Note that cysteine is easily oxidized to cystine, therefore detection of cystine in the culture medium is not unexpected. Removing pyruvate from the culture medium had no significant influence on the metabolites in the absence of UVA. However, the lack of pyruvate during irradiation resulted in increased glutamate release and decrease in cystine consumption (Figure S. 4b and c respectively). Pyruvate had no influence on the consumption of glutamine with or without irradiation (Supplementary Figure S. 4a).

2.3 Non-enzymatic conversion of pyruvate to acetate upon ROS treatment with H₂O₂ or UVA

It has been shown that pyruvate could have antioxidant properties and could be converted to acetate in a ROS dependent manner [17–20]. Furthermore, there have been studies indicating a non-enzymatic decarboxylation of pyruvate to acetate in the presence of reactive oxygen species (H₂O₂) [23–25]. Since we have observed a decrease in pyruvate release and increase in acetate secretion after UVA treatment (Fig. 2c) we aimed to validate that UVA treatment can also result in the non-enzymatic decarboxylation of pyruvate. In our experimental setup, we treated pyruvate dissolved in water with H₂O₂ or UVA and measured the decomposition of pyruvate to acetate. When pyruvate is treated with 100 μ M H₂O₂ or 6 J/cm²

UVA irradiation, in both cases it is non-enzymatically converted to acetate (Fig. 3a and b respectively).

2.4 Pyruvate detoxifies UVA-induced ROS but does not offer full protection against ROS-induced DNA damage

Since we observed UVA-induced non-enzymatic decarboxylation of pyruvate to acetate (Fig. 3b), and changes in other key metabolites (Supplementary Figure S. 4), with a potential role in ROS detoxication, we aimed to test whether the presence of pyruvate has antioxidant and DNA-protective effects during UVA irradiation. To test the antioxidant capacity of pyruvate, fibroblasts were treated with and without 6 J/cm² UVA irradiation (single irradiation dose; for treatment protocol see Supplementary Figure S. 1b) with and without 1 mM pyruvate present in the medium. Subsequent measurement of ROS showed that in the presence of pyruvate the amount of ROS is significantly reduced (Fig. 4a).

To test whether pyruvate can protect against UVA-induced 8-hydroxydeoxyguanosine mutations (8-OHdG), cells were UVA-irradiated repeatedly with 6 J/cm² over a period of 2 or 4 days with and without 1 mM pyruvate in the medium. After four days of treatment, human fibroblasts showed no difference in 8-OHdG levels between irradiated and non-irradiated samples (Supplementary Figure S. 5). Two days of UVA-treatment resulted in the formation of 8-OHdG (Fig. 4b). Pyruvate addition to the medium (1 mM) alleviated the effects of endogenously produced 8-OHdG in the absence of UVA but had no effect on DNA damage when the cells were subjected to UVA irradiation (Fig. 4b).

2.5 UVA and pyruvate influence MMP expression

Matrix metalloproteases are important players in photoaging and photo carcinogenesis. In our experimental setup, primary human fibroblasts were irradiated with repetitive sub-erythema doses UVA (3 \times daily for 4 days, 6 J/cm² per irradiation) and the expression of four MMPs was measured—MMP1, MMP2, MMP3, and MMP15. The MMPs

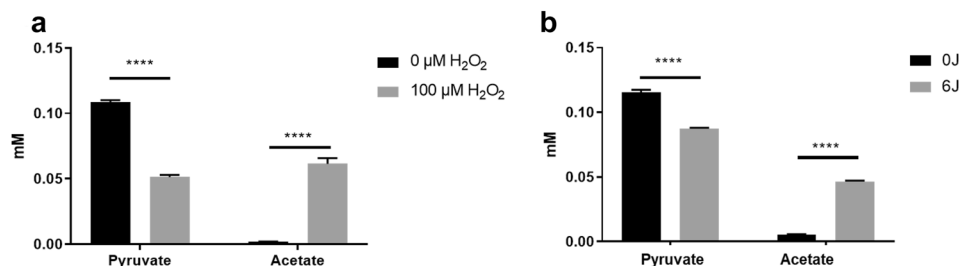


Fig. 3 Pyruvate (100 μ M) can be non-enzymatically decarboxylated to acetate in water after the addition of an equimolar amount of H₂O₂ (a) or UVA irradiation (b). (Statistical analysis: Two-way ANOVA

with Bonferroni's multiple comparisons test, (****) $P < 0.0001$) J Joule, H₂O₂ hydrogen peroxide, μ M micromolar

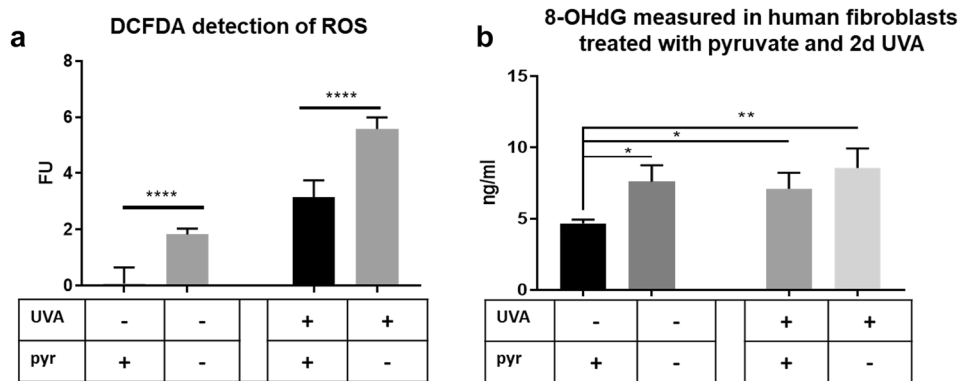
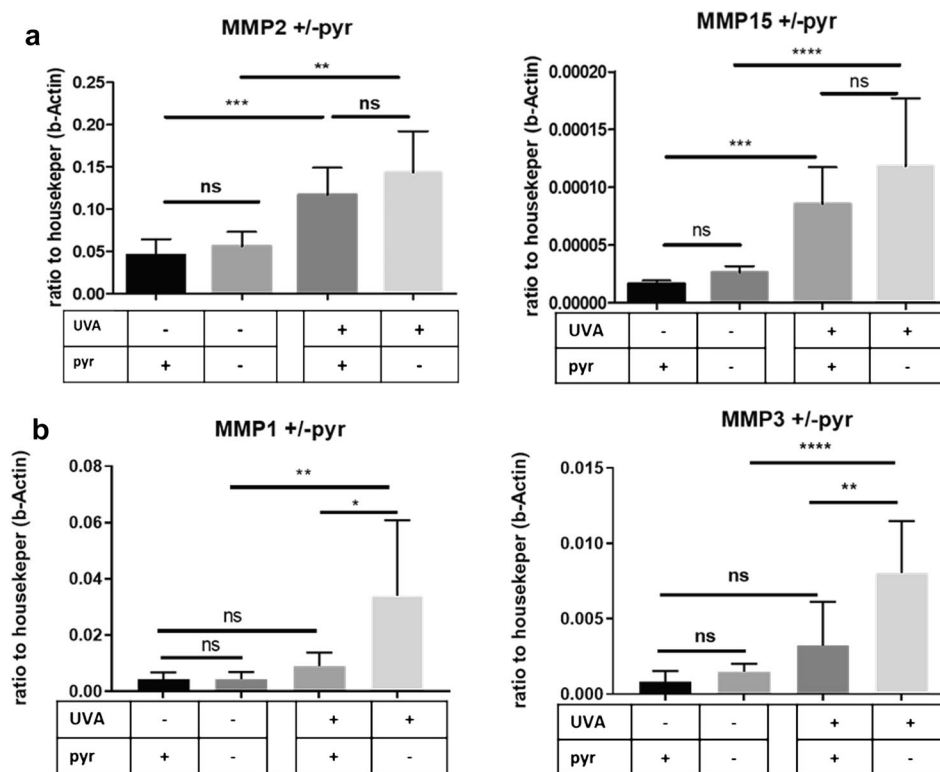


Fig. 4 Antioxidant properties of pyruvate. Addition of 1 mM pyruvate to the cell culture medium reduces the amount of reactive oxygen species (ROS) (a), produced by UVA and subsequently decreases ROS-induced DNA 8-OHdG damage in human fibroblasts (b). (Sta-

tistical analysis: Two-way ANOVA with Bonferroni's multiple comparisons test, For significances: (*) $P < 0.05$; (**) $P < 0.005$; (****) $P < 0.0001$) *pyr* pyruvate, *2d* two days, *8-OHdG* 8-hydroxydeoxyguanosine

Fig. 5 Upon treatment, MMP2 and MMP15 showed UVA-dependent increase but pyruvate had no significant influence on mRNA expression (a). In comparison, the presence of pyruvate in the cell culture medium decreases the expression of matrix metalloproteases (MMPs) MMP1 and MMP3 in irradiated samples, compared to controls without pyruvate (b). (Statistical analysis: Two-way ANOVA with Bonferroni's multiple comparisons test, For significances: (ns) $P > 0.05$; (*) $P < 0.05$; (**) $P < 0.005$; (***) $P < 0.0005$; (****) $P < 0.0001$) *pyr* pyruvate, *ns* not significant



could be subsequently divided in two distinct groups in accordance with their reaction to UVA treatment and pyruvate content in the medium. The first group, consisting of MMP2 and MMP15 (Fig. 5a), showed UVA-induced upregulation. The lack of pyruvate in the medium, on the other hand, resulted in no significant changes in MMP2 or MMP15 expression in both irradiated and un-irradiated cells when compared to the pyruvate-containing controls. The second MMP group, consisting of MMP1 and MMP3 (Fig. 5b), showed no UVA-regulation when cultured in

pyruvate (1 mM). However, the absence of pyruvate from the medium during irradiation lead to significant increase in expression for both MMP1 and MMP3 (Fig. 5b).

3 Discussion

As previously published by Kamenisch et al. [13], UVA irradiation induces increased glucose consumption and lactate production in melanoma cells. In the case of

melanoma, UVA irradiation can be beneficial for tumor growth via increased lactate production, which in turn can promote immune attenuation and escape of tumor cells from the immune system [26–28].

But UV-induced lactate production can also be beneficial for non-malignant skin tissue. There is evidence that UVA-radiation and the resulting DNA damage can initiate immune response [29, 30]. The increased lactate secretion of irradiated healthy fibroblasts could help to facilitate immediate attenuation of UV-induced immune cells [26, 27, 31], thereby lowering the risk of auto-immune reactions during regular sun exposure of normal skin.

Another known effect of lactate is the enhancement of MMP expression [13], thus contributing to neo-vascularization and tumor dissemination. Furthermore, tumor cells can implement aerobic glycolysis as means for alternative energy production and also in case of mitochondrial damage caused by UVA irradiation [12, 32, 33].

In our current study, we have shown that UVA-induced metabolic changes are not limited to malignant skin cells. Repetitive sub-erythema doses of UVA [34] applied on primary human fibroblasts resulted in a metabolic profile, which is similar to the one we observed in melanoma cells. This is, to our knowledge, the first time such metabolic effect of sub-erythema doses of UVA has been observed in primary human fibroblasts. In 2014 Marionnet et al. published an article showing an increase of glucose-metabolism-related genes in UVA irradiated keratinocytes but not in fibroblasts [16]. In addition to this, the single high dose applied by Marionnet et al. (higher than the minimal erythema dose (MED) measured for UVA [34]) is different from the repetitive sub-MED dose radiation used in our experiments. Single high doses of radiation (e.g. 40 J/cm² [16]) can induce different cellular responses than sub-MED dose, repetitive radiation, which can be compared to moderate sun exposure of human skin.

Besides lactate associated immune suppression, it is possible that these large extents of metabolic changes in glucose, pyruvate and lactate upon UVA treatment could be associated to the detoxification of UVA-induced ROS. As we observed increase in lactate release by primary fibroblasts, it should be noted that this metabolite has been known to have certain antioxidant properties [35]. A potential function as extra-cellular antioxidant could explain the need for the cells to secrete lactate in greater quantities after irradiation (Fig. 1b).

In accordance with earlier publications [23, 25], we have verified that pyruvate dissolved in water is non-enzymatically decarboxylated to acetate upon H₂O₂ treatment and a similar reaction could be observed when pyruvate was treated with UVA as another ROS source (Fig. 3a, b). The ability of pyruvate to react with ROS and be decarboxylated to acetate is supported by our findings

in fibroblasts (Fig. 2c). Furthermore in the presence of sufficient pyruvate, this metabolite can be consumed by ROS, as indicated by the increased consumption of pyruvate upon irradiation (Fig. 2a). In the case of no pyruvate supplementation, the cell has to produce pyruvate and has to release it to prevent accumulation of extracellular ROS, thus lowering the oxidative stress burden by the environment (Fig. 2b). After UVA treatment, a part of this produced and released pyruvate is consumed by ROS (Fig. 2b). Taken together, these data indicate, that cellular release of pyruvate or supplemented pyruvate in the medium can be used as ROS detoxification agent during treatment with a ROS source.

In the context of ROS detoxification, we investigated additional metabolites that play important roles in the cellular oxidative defense, namely glutamine, glutamate, and cystine [36, 37]. UVA resulted in increase of glutamine and cystine consumption (see Supplementary Figures S. 4a and 4c). The increase in cystine consumption after irradiation also correlates with increase in glutamate release (Supplementary Figure S. 4b), which can be attributed to an active glutamate/cystine antiporter [38].

However, the absence of pyruvate during irradiation led to a decrease in cystine consumption, which could be interpreted as reduction of cellular ROS-defense. This supports the notion that pyruvate might be crucial for first-line defense during oxidative stress, giving the cells enough time to implement further antioxidant strategies. Glutamate secretion, however, further increases when the cells are treated with UVA in the absence of pyruvate. There has been evidence that glutamate can act as an autocrine proliferation signaling molecule [37]. It is possible that the increase in glutamate secretion is connected to the prevention of apoptosis and allows the fibroblasts to proliferate even after irradiation (as seen in Supplementary Figure S. 3).

As shown by us and others, pyruvate has antioxidant properties [17, 19, 23]. However, extracellular pyruvate does not seem to protect completely from UVA-induced DNA damage. It is possible that the experimental setup with repetitive UVA irradiation, in combination with the used sub-MED UVA doses, leads to an equilibrium in the damage-repair processes in the cells where the addition of stressor does not lead to an increased damage, similar to the equilibrium described by Zaharieva et al. [39]. This is supported by the fact that after a complete irradiation cycle (4 days, 3 × irradiation per day) no significant difference between irradiated and un-irradiated cells in terms of 8-OHdG (Supplementary Figure S. 5) can be seen. The increase of DNA damage detected in un-irradiated cells between 2d (Fig. 4) and 4d (Supplementary Figure S. 5) is likely to come from increased endogenous ROS due to cell handling (changes in CO₂ concentrations between incubator and cell culture room, mechanical stress due to medium exchange, etc.).

Pyruvate could, nevertheless, limit endogenous 8-OHdG formation in un-irradiated cells compared to un-irradiated cells cultured without pyruvate. This supports the theory that pyruvate could play a role as a first line of defense against UVA-induced oxidative stress, providing immediate but mild protection and the time to initiate other antioxidant defenses.

As seen from our experiments, primary human fibroblasts showed glucose consumption and lactate production profiles after irradiation similar to the ones previously observed in melanoma cells [13]. Kamenisch et al. have identified lactic acid as one important mediator of UV-induced MMP induction in these cells [13]. In our current experiments we observed that UVA irradiation also upregulates MMP expression in human fibroblasts. From the MMPs investigated here (MMP1, MMP2, MMP3, and MMP15), especially MMP1, MMP2, and MMP3 are key players in the complex process of skin aging, especially in photoaging [40, 41]. It has to be noted that these MMPs can also play a role in photocarcinogenesis [40], enhancing invasion and migration of tumor cells. Therefore, the UVA-induced secretion of MMPs in the dermal matrix from fibroblasts could also promote migration of initial tumor cells in the skin, which could be attenuated by high pyruvate concentrations. Concerning MMP15, there is still little information available on its expression pattern and regulation to give insights to its role in photoaging and its association with pyruvate.

In the current work, two of the tested MMPs – MMP1 and MMP3, showed a tendency of increased gene expression when the cells were irradiated with UVA under 1 mM pyruvate conditions, but the expression upregulation was not statistically significant. However, without the addition of pyruvate a significant upregulation was observed for both MMPs (Fig. 5b). This behavior points in similar direction as previously reported findings [42–44] where UVA leads to significant upregulation of these MMPs. The ability of pyruvate to regulate the expression of MMP1 and MMP3 has been previously reported by Kim et al. [22]. However, in their publication, Kim and associates use much longer treatment periods (12 days) compared to our treatment protocol (4 days). Furthermore, their publication does not provide connection between an external ROS-inducer (such as UVA) and pyruvate. To our knowledge, we are the first to date to show that pyruvate attenuates the UVA-induced upregulation of MMP1 and MMP3.

In the case of MMP2, UVA irradiation under normal cell culture conditions (1 mM pyruvate), resulted in increase of expression in accordance with previously published data [21, 40]. The absence of pyruvate during irradiation lead to visible but not statistically significant increase of MMP2 expression when compared to cells irradiated with 1 mM pyruvate (Fig. 5a). As recently described by us [21], MMP15 again showed increase in expression after UVA irradiation. Supplementation with pyruvate showed slight,

but not significant, reduction of the UVA effects on MMP15 expression. Interestingly, the absence of pyruvate in non-irradiated cell also resulted in a visible, albeit statistically not significant, increase in MMP15 expression. This behavior is similar to the one observed by Kim and associates for MMP1 and MMP3 [22], but, to our knowledge, has never before been observed for MMP15.

The collected data show that pyruvate has a significant protective potential against photoaging associated expression of MMPs (Fig. 5). This link between pyruvate and skin aging opens new aspects of the metabolic influence on skin aging. It would be interesting if to see if local pyruvate concentrations in the skin are low in individuals where skin aging progresses faster with a larger extent of wrinkle formation and loss of skin elasticity. Therefore, our data could serve as a basis for further in vivo studies on the potential of pyruvate as a cosmetic and therapeutic additive in topical applications aiming to reduce ROS and wrinkle formation.

4 Conclusion

Similar to melanoma cells, primary human fibroblasts show increased glucose consumption and lactate production. Further metabolic changes after irradiation support the role of pyruvate as a first-line antioxidant defense during UVA challenge. In addition, sufficient pyruvate can protect non-malignant cells against UVA-induced ROS, DNA damage and photoaging-related expression of MMP1 and MMP3. This opens the door for further studies concerning the clinical application of pyruvate as potential antioxidant, and inhibitor of MMP expression.

5 Materials and methods

5.1 Cell culture

Skin biopsy sample was obtained from the University Hospital Regensburg (Ethic vote number 14101 0001) and given the designation Re5. The skin biopsy was put whole on a Primaria cell culture dish (#353801, Corning, Germany), containing a single drop of DMEM-Cipro medium (DMEM medium (P04-01548, PAN Biotech, Germany) containing 10% FCS (AC-SM-0161, Anprotec, Germany), 1 g/L (5.5 mM) glucose (G8644, Sigma-Aldrich/Merck, Germany), 1 mM pyruvate (#11360070, Thermo Fischer, Germany), 2 mM L-glutamine (G7513, Sigma-Aldrich/Merck, Germany) and 1% Ciprofloxacin (200 mg/100 ml infusion solution, 64,689.00.00, Fresenius Kabi, Germany)) and incubated for 30 min at 37 °C to ensure that the skin sample sticks on the dish surface. Afterward, 3 ml DMEM-Cipro

was added to the skin sample. It was cultivated at 37°, 5% CO₂ until fibroblast-outgrowth was enough for a transfer to a T25 cell culture flask where they were cultured in DMEM without Ciprofloxacin, and used for further experiments.

Before irradiation, the cells were seeded at density of 5×10^4 cells per well on a 6-well plate in DMEM with and without pyruvate (1 mM/0 mM) and incubated overnight.

5.2 Two in one cell count and viability test

To determine the number of cells, as well as their viability, a LUNA-FL Dual Fluorescence Cell Counter (Logos Biosystems, Aligned Genetics, Inc., Korea) in combination with Acridine orange/Propidium iodide (AO/PI) staining was used. To perform the actual cell-count, 18 µL of cell suspension were mixed with 2 µL AO/PI dye (F23001-LG, BioCat, Germany). From this mixture, 10 µL was pipetted on LUNA cell counting slides and measured in fluorescence modus with LUNA-FL.

5.3 UVA irradiation

At the beginning of irradiation, the medium was aspirated from each well. Cells were irradiated in 1 mL PBS (#14190094, Thermo Fisher, Germany,). For graphical representation of the irradiation protocol see Supplementary Figure S1 a. The amount of UVA per single irradiation was set at 6 J/cm² and provided by a Sellamed-Lamp (Sellas Medizinische Geräte GmbH, Germany) with emission spectrum 340–420 nm (see Supplementary Figure S2). The PBS was then aspirated and 5 mL fresh medium was added to each well after the first irradiation. Before all subsequent irradiations, the medium was aspirated and collected in separate falcons and returned to the corresponding wells afterward. There were a total of 3 irradiations per day with a 4 h resting period between each irradiation and an overnight rest after the final daily irradiation.

5.4 Metabolic analysis—NMR

After the UVA treatment, the supernatant from the cell samples as well as control media without cells was preserved at – 80 °C before further preparation. In preparation for the NMR measurements, 400 µL from each sample were mixed with 200 µL of 0.1 M phosphate buffer, pH 7.4, which contained in addition 3.9 mM boric acid to impair the growth of bacteria in the sample and 50 µL of 0.75 (wt) trimethylsilylpropanoic acid (TSP; Sigma-Aldrich, Germany) in deuterium oxide (D₂O) as internal reference standard and pipetted in glass NMR-vials. Additionally, 10 µL of 81.97 mmol/L formic acid (FA) were added as a second internal reference standard that is not prone to protein binding.

To validate the ability of UVA to non-enzymatically decarboxylate pyruvate to acetate, 100 µM pyruvate,

corresponding to the physiological pyruvate concentration in human blood, were dissolved in double distilled water and irradiated with a single UVA dose (6 J/cm²). As a control, the same amount of pyruvate was dissolved in water and mixed with 100 µM H₂O₂. The resulting samples were prepared for NMR analysis as described above. Since there were no proteins in the mixture to disturb the NMR measurement, no FA was added.

All NMR experiments were performed at 298 K on a 600 MHz Bruker Avance III HD spectrometer (Bruker BioSpin GmbH, Germany) using a triple resonance (¹H, ¹³C, ¹⁵N, ²H lock) cryogenic probe with z-gradients in combination with a Bruker SampleJet sample changer (Bruker BioSpin GmbH, Germany).

Spectra of cell culture supernatants and control media were acquired employing a 1D ¹H Carr-Purcell-Meiboom-Gill (CPMG) pulse sequence to achieve effective suppression of macromolecular signals. These broad macromolecular signals, if not suppressed, overlap with signals of small molecules and hamper their identification and quantification. Due to their size macromolecules such as proteins tumble in solution much slower than small molecules. As a result, the T₂ relaxation times that determine the time span in which an NMR signal may be observed are much smaller for macromolecules than for small molecules such as typical metabolites. Therefore, employing a T₂ relaxation filter as incorporated in the CPMG pulse sequence allows efficient suppression of macromolecular signals, whereas signals of small molecules are only minimally impacted. This leads to clean 1D proton NMR spectra in which metabolite identification and quantification is considerably eased.

The acquired data were semi-automatically Fourier-transformed to 128 k real data points, phase corrected and baseline optimized with TopSpin 4.0.7 (Bruker BioSpin GmbH). Chenomx 8.6 (Chenomx Inc., AB, Canada) was employed for final quantification of metabolites from 1D NMR spectra. The concentration of metabolites in the cell supernatants (*C_s*) and in fresh medium (*C_{med}*) were used together with the sample volume (*vol_s*) used in the 6 well plates used for cell culture—5 mL, and the end number of cells to calculate metabolites per million cells. For that, the following equation was used:

$$\text{mmol}/10^6 \text{ cells} = \frac{(C_{med} * \text{AVERAGE } vol_s [L]) - (C_s * vol_s [L])}{10^6 \text{ cells}}$$

5.5 DCFDA-ROS detection

Cells were seeded on a 10 cm dish at density of 5×10^5 cells per dish in DMEM with or without pyruvate, and cultured for 2 days at 37 °C. Afterward, the dishes were washed 1 × with DMEM without FCS. From that point all remaining steps were performed in the dark. The cells were stained with

Table 1 Product size and annealing temperatures of the used primers (Sigma-Aldrich, Germany)

Gene of interest	Primer sequence: forward/reverse	Size of product (bp—base pairs)	Annealing temperature
MMP1	TCACCAAGGTCTCTGAGGGTCAAGC/GGATGCCATCAATGTCATCCTGAGC	324 bp	65 °C
MMP2	CCCCAAAACGGACAAAGAG/CTTCAGCACAAACAGGTTGC	88 bp	54 °C
MMP3	CAAAACATATTTCTTTGTAGAGAGGACAA/ TTCAGCTATTTGCTTGGGGAAA	91 bp	54 °C
MMP15	ACGGTCGTTTTGTCTTTTCA/GTCAGCGGCTGTGGGTAG	85 bp	57 °C
b-Actin	CTACGTCGCCCTGGACTTCGAGC/GATGGAGCCGCCGATCCACACGG	385 bp	54–65 °C

100 μ M DCFDA (from a 10 mM stock in DMSO, D6883, Sigma-Aldrich/Merck, Germany), dissolved in DMEM without FCS, and incubated for 35 min at 37 °C. Some cells were left unstained to be later used as background control. After the end of incubation, the cells were washed 2 \times with medium without FCS, trypsinized, counted, and transferred to two black clear bottom 96well plates at density 1×10^4 cells per well in a total volume of 100 μ L per well. One plate was left as 0 J non-irradiated control and the other one was immediately irradiated with a single dose of 6 J/cm² UVA to induce ROS. After the irradiation, both plates were incubated for 30 min at 37 °C in the dark. Fluorescence was measured via Varioscan at Ex/Em 485 nm/530 nm. (For graphical representation of the treatment see Supplementary Figure S. 1b).

5.6 DNA extraction and detection of 8-OHdG

In order to retrieve DNA for subsequent 8-OHdG experiments, UVA treated cells and controls (for standard irradiation protocol see Supplementary Figure S. 1a), cultured on 20 cm Petri dishes at a seeding density of 8×10^5 cells per petridish, were trypsinized, centrifuged, and re-suspended in 200 μ L/sample PBS. From then on, a QUIamp Mini Kit (#51306, QIAGEN, USA) was used for the isolation.

The method used to detect oxidative DNA damage in UVA-irradiated cells was based on the OxiSelect™ ELISA Kit (STA-320, Cell Biolabs Inc., USA). This kit is a competitive enzyme immunoassay for the detection and quantitation of 8-OHdG in DNA samples.

5.7 RNA extraction and qPCR

RNA extraction from the treated cells was performed via NucleoSpin RNA-isolation kit (# 740955.250, Machery-Nagel, Germany) in accordance with the manufacturer's protocol. The concentration of RNA in the samples as determined via NanoDrop. For the reverse transcription, 500 ng RNA per sample was used. A master mix was prepared for the reverse transcription, containing 1 μ L random primer (#11034731001, Roche, Germany), 4 μ L 5 \times buffer (SuperScript II, # 18064-014 Invitrogen/Thermo Fisher, Germany),

1 μ L dNTPs (N0446S, New England Bio Labs, Germany), 1 μ L DTT (SuperScript II, # 18064-014 Invitrogen/Thermo Fisher, Germany), and 2 μ L water per sample. Up to 10 μ L RNA was added to the mix and the rest of the volume up to 19 μ L was filled with water. The RNA was stretched for 10 min at 70 °C. Afterward, 1 μ L SuperScript enzyme (SuperScript II, # 18064-014 Invitrogen/Thermo Fisher, Germany) was added to each sample at room temperature followed by 45 min incubation at 42 °C and subsequently 10 min at 70 °C. At the end of the reverse transcription, the samples were cooled and stored at 4 °C.

For the qPCR analysis, each sample contained 10 μ L SybrGreen (#06924204001, Roche, Germany), 0.5 μ L forward primer, 0.5 μ L reverse primer, 8 μ L water, and 1 μ L cDNA. For the negative control, 1 μ L water was used instead of cDNA. 20 μ L from each sample were pipetted in duplicates on a 96-well LightCycler plate (#04729692001, Roche, Germany). Optimal annealing temperatures were determined for each gene of interest as shown in Table 1. The qPCR reaction was performed in Roche LightCycler 96 (Roche, Germany), programmed for 45 cycles of amplification.

The end results were calculated with LightCycler 96 software and presented as a ratio to the housekeeper (b-actin).

5.8 Statistical analysis

Data are shown as the mean with standard deviation of at least three independent experiments and statistical significance was tested with two-way ANOVA with Bonferroni's multiple comparisons post-test analysis (a P value < 0.05 was considered significant). Statistical analysis was performed with GraphPad Prism 10 (GraphPad, USA).

Supplementary Information The online version contains supplementary material available at <https://doi.org/10.1007/s43630-023-00419-z>.

Author contributions II, CB, WG, MK, TM, BK, YK and MB have substantially contributed to this manuscript. II and YK wrote the paper with the help of MB, WG, MK, BK and TM; performed literature research, analyzed literature data and developed the hypothesis. II designed the experiments with the help of WG, MK, YK and MB. II

conducted the experiments and made the figures with the help of CB and BK. All authors approved the versions of the manuscript.

Funding Open Access funding enabled and organized by Projekt DEAL. This work was partially funded by the Deutsche Forschungsgemeinschaft (DFG) Klinische Forschergruppe KFO 262, Project 11.

Availability of data and material Detailed information about used materials, methods and data are available upon request.

Code availability Not applicable.

Declarations

Conflict of interest The authors have no conflict of interest.


Open Access This article is licensed under a Creative Commons Attribution 4.0 International License, which permits use, sharing, adaptation, distribution and reproduction in any medium or format, as long as you give appropriate credit to the original author(s) and the source, provide a link to the Creative Commons licence, and indicate if changes were made. The images or other third party material in this article are included in the article's Creative Commons licence, unless indicated otherwise in a credit line to the material. If material is not included in the article's Creative Commons licence and your intended use is not permitted by statutory regulation or exceeds the permitted use, you will need to obtain permission directly from the copyright holder. To view a copy of this licence, visit <http://creativecommons.org/licenses/by/4.0/>.

References

1. Modenese, A., Korpinen, L., & Gobba, F. (2018). Solar radiation exposure and outdoor work: An underestimated occupational risk. *International Journal of Environmental Research and Public Health*, 15(10), 2063. <https://doi.org/10.3390/ijerph15102063>
2. Armstrong, B., Baverstock, K., Brenner, D., Cardis, E., Green, A., Guilmette, R., Hall, J., Hill, M., Hoel, D., Krewski, D., Little, M., Marshall, M., Mitchel, R., Muirhead, C., Priest, N., Richardson, D., Riddell, T., Sabatier, L., Sokolnikov, M., & Ullrich, R. (2012). PartD: Radiation. Volume 100. A review of human carcinogens. *IARC monographs on the evaluation of carcinogenic risks to humans*. 100. pp. 35–40
3. Parisi, A. V., & Wong, J. C. F. (1997). Erythral irradiances of filtered ultraviolet radiation. *Physics in Medicine and Biology*, 42(7), 1263–1275. <https://doi.org/10.1088/0031-9155/42/7/003>
4. Kimlin, M. G., & Parisi, A. V. (1999). Ultraviolet radiation penetrating vehicle glass: A field based comparative study. *Physics in Medicine and Biology*, 44(4), 917–926. <https://doi.org/10.1088/0031-9155/44/4/008>
5. Jaszewska, E., Soin, M., Filipek, A., & Naruszewicz, M. (2013). UVA-induced ROS generation inhibition by *Oenothera paradoxa* defatted seeds extract and subsequent cell death in human dermal fibroblasts. *Journal of Photochemistry and Photobiology B: Biology*, 126, 42–46. <https://doi.org/10.1016/j.jphotobiol.2013.07.001>
6. Ichihashi, M., Ueda, M., Budiyanto, A., Bito, T., Oka, M., Fukunaga, M., Tsuru, K., & Horikawa, T. (2003). UV-induced skin damage. *Toxicology*, 189(1), 21–39. [https://doi.org/10.1016/S0300-483X\(03\)00150-1](https://doi.org/10.1016/S0300-483X(03)00150-1)
7. Seifermann, M., & Epe, B. (2017). Oxidatively generated base modifications in DNA: Not only carcinogenic risk factor but also regulatory mark? *Free Radical Biology and Medicine*, 107, 258–265. <https://doi.org/10.1016/j.freeradbiomed.2016.11.018>
8. Birch-Machin, M. A., & Bowman, A. (2016). Oxidative stress and ageing. *British Journal of Dermatology*, 175, 26–29. <https://doi.org/10.1111/bjd.14906>
9. Jéquier, E. (1994). Carbohydrates as a source of energy. *American Journal of Clinical Nutrition*, 59(3 Suppl), 682s–685s. <https://doi.org/10.1093/ajcn/59.3.682S>
10. Vander Heiden, M. G., Cantley, L. C., & Thompson, C. B. (2009). Understanding the Warburg effect: The metabolic requirements of cell proliferation. *Science*, 324(5930), 1029–1033. <https://doi.org/10.1126/science.1160809>
11. Abdel-Haleem, A. M., Lewis, N. E., Jamshidi, N., Mineta, K., Gao, X., & Gojobori, T. (2017). The emerging facets of non-cancerous Warburg effect. *Frontier Endocrinology (Lausanne)*, 8, 279. <https://doi.org/10.3389/fendo.2017.00279>
12. Warburg, O., Wind, F., & Negelein, E. (1927). The metabolism of tumors in the body. *Journal of General Physiology*, 8(6), 519–530.
13. Kamenisch, Y., Baban, T. S., Schuller, W., von Thaler, A. K., Sinnberg, T., Metzler, G., Bauer, J., Schitteck, B., Garbe, C., Rocken, M., & Berneburg, M. (2016). UVA-irradiation induces melanoma invasion via the enhanced Warburg effect. *Journal of Investigative Dermatology*, 136(9), 1866–1875. <https://doi.org/10.1016/j.jid.2016.02.815>
14. Yang, X., Wang, J., Wang, H., Li, X., He, C., & Liu, L. (2021). Metabolomics study of fibroblasts damaged by UVB and BaP. *Scientific Reports*, 11(1), 11176. <https://doi.org/10.1038/s41598-021-90186-7>
15. Kremslehner, C., Miller, A., Nica, R., Nagelreiter, I.-M., Narzt, M.-S., Golabi, B., Vorstandlechner, V., Mildner, M., Lachner, J., Tschachler, E., Ferrara, F., Klavins, K., Schosserer, M., Grillari, J., Haschemi, A., & Gruber, F. (2020). Imaging of metabolic activity adaptations to UV stress, drugs and differentiation at cellular resolution in skin and skin equivalents—Implications for oxidative UV damage. *Redox Biology*, 37, 101583. <https://doi.org/10.1016/j.redox.2020.101583>
16. Marionnet, C., Pierrard, C., Golebiewski, C., & Bernerd, F. (2014). Diversity of biological effects induced by longwave UVA rays (UVA1) in reconstructed skin. *PLoS ONE*, 9(8), e105263. <https://doi.org/10.1371/journal.pone.0105263>
17. O'Donnell-Tormey, J., Nathan, C., Lanks, K., DeBoer, C., & Harpe, J. (1987). Secretion of pyruvate An antioxidant defense of mammalian cell. *The Journal of Experimental Medicine*, 165, 500–514.
18. Mallet, R. T., Squires, J. E., Bhatia, S., & Sun, J. (2002). Pyruvate restores contractile function and antioxidant defenses of hydrogen peroxide-challenged myocardium. *Journal of Molecular and Cellular Cardiology*, 34(9), 1173–1184. <https://doi.org/10.1006/jmcc.2002.2050>
19. Ramos-Ibeas, P., Barandalla, M., Colleoni, S., & Lazzari, G. (2017). Pyruvate antioxidant roles in human fibroblasts and embryonic stem cells. *Molecular and Cellular Biochemistry*, 429(1), 137–150. <https://doi.org/10.1007/s11010-017-2942-z>
20. Aoki-Yoshida, A., Aoki, R., & Takayama, Y. (2013). Protective effect of pyruvate against UVB-induced damage in HaCaT human keratinocytes. *Journal of Bioscience and Bioengineering*, 115(4), 442–448. <https://doi.org/10.1016/j.jbiosc.2012.11.004>
21. Ivanova, I., Kurz, B., Lang, K., Maisch, T., Berneburg, M., & Kamenisch, Y. (2022). Investigation of the HelioVital filter foil revealed protective effects against UVA1 irradiation-induced DNA damage and against UVA1-induced expression of matrixmetalloproteinases (MMP) MMP1, MMP2, MMP3 and MMP15. *Photochemical and Photobiological Sciences*, 21(3), 361–372. <https://doi.org/10.1007/s43630-022-00177-4>
22. Kim, J. Y., Lee, S. H., Bae, I.-H., Shin, D. W., Min, D., Ham, M., Kim, K.-H., Lee, T. R., Kim, H.-J., Son, E. D., Lee, A.-Y., Song, Y. W., & Kil, I. S. (2018). Pyruvate protects against cellular senescence through the control of mitochondrial and lysosomal function in dermal fibroblasts. *Journal of Investigative Dermatology*, 138(12), 2522–2530. <https://doi.org/10.1016/j.jid.2018.05.033>

23. Constantopoulos, G., & Barranger, J. A. (1984). Nonenzymatic decarboxylation of pyruvate. *Analytical Biochemistry*, 139(2), 353–358. [https://doi.org/10.1016/0003-2697\(84\)90016-2](https://doi.org/10.1016/0003-2697(84)90016-2)
24. Lopalco, A., Dalwadi, G., Niu, S., Schowen, R. L., Douglas, J., & Stella, V. J. (2016). Mechanism of decarboxylation of pyruvic acid in the presence of hydrogen peroxide. *Journal of Pharmaceutical Sciences*, 105(2), 705–713. <https://doi.org/10.1002/jps.24653>
25. Drachman, N., Kadlecsek, S., Duncan, I., & Rizi, R. (2017). Quantifying reaction kinetics of the non-enzymatic decarboxylation of pyruvate and production of peroxydicarbonate with hyperpolarized ¹³C-NMR. *Physical Chemistry Chemical Physics*, 19(29), 19316–19325. <https://doi.org/10.1039/C7CP02041D>
26. Fischer, K., Hoffmann, P., Voelkl, S., Meidenbauer, N., Ammer, J., Edinger, M., Gottfried, E., Schwarz, S., Rothe, G., Hoves, S., Renner, K., Timischl, B., Mackensen, A., Kunz-Schughart, L., Andreesen, R., Krause, S. W., & Kreutz, M. (2007). Inhibitory effect of tumor cell-derived lactic acid on human T cells. *Blood*, 109(9), 3812–3819. <https://doi.org/10.1182/blood-2006-07-035972>
27. Gottfried, E., Kunz-Schughart, L. A., Ebner, S., Mueller-Klieser, W., Hoves, S., Andreesen, R., Mackensen, A., & Kreutz, M. (2006). Tumor-derived lactic acid modulates dendritic cell activation and antigen expression. *Blood*, 107(5), 2013–2021. <https://doi.org/10.1182/blood-2005-05-1795>
28. Siska, P. J., Singer, K., Evert, K., Renner, K., & Kreutz, M. (2020). The immunological Warburg effect: Can a metabolic-tumor-stroma score (MeTS) guide cancer immunotherapy? *Immunological Reviews*, 295(1), 187–202. <https://doi.org/10.1111/imr.12846>
29. Schneider, L. A., Raizner, K., Wlaschek, M., Brenneisen, P., Gethöffer, K., & Scharffetter-Kochanek, K. (2017). UVA-1 exposure in vivo leads to an IL-6 surge within the skin. *Experimental Dermatology*, 26(9), 830–832. <https://doi.org/10.1111/exd.13286>
30. Gekara, N. O. (2017). DNA damage-induced immune response: Micronuclei provide key platform. *Journal of Cell Biology*, 216(10), 2999–3001. <https://doi.org/10.1083/jcb.201708069>
31. Kanemaru, H., Mizukami, Y., Kaneko, A., Tagawa, H., Kimura, T., Kuriyama, H., Sawamura, S., Kajihara, I., Makino, K., Miyashita, A., Aoi, J., Makino, T., Masuguchi, S., Fukushima, S., & Ihn, H. (2021). A mechanism of cooling hot tumors: Lactate attenuates inflammation in dendritic cells. *iScience*, 24(9), 103067. <https://doi.org/10.1016/j.isci.2021.103067>
32. Warburg, O. (1956). On respiratory impairment in cancer cells. *Science*, 124(3215), 269–270.
33. Djavaheri-Mergny, M., Marsac, C., Mazière, C., Santus, R., Michel, L., Dubertret, L., & Mazière, J. C. (2001). UV-A irradiation induces a decrease in the mitochondrial respiratory activity of human NCTC 2544 keratinocytes. *Free Radical Research*, 34(6), 583–594. <https://doi.org/10.1080/10715760100300481>
34. Welti, M., Ramelyte, E., Dummer, R., & Imhof, L. (2020). Evaluation of the minimal erythema dose for UVB and UVA in context of skin phototype and nature of photodermatosis. *Photodermatology, Photoimmunology and Photomedicine*, 36(3), 200–207. <https://doi.org/10.1111/phpp.12537>
35. Groussard, C., Morel, I., Chevanne, M., Monnier, M., Cillard, J., & Delamarche, A. (2000). Free radical scavenging and antioxidant effects of lactate ion: An in vitro study. *Journal of Applied Physiology*, 89(1), 169–175. <https://doi.org/10.1152/jappl.2000.89.1.169>
36. Raj Rai, S., Bhattacharyya, C., Sarkar, A., Chakraborty, S., Sircar, E., Dutta, S., & Sengupta, R. (2021). Glutathione: Role in oxidative/nitrosative stress, antioxidant defense, and treatments. *ChemistrySelect*, 6(18), 4566–4590. <https://doi.org/10.1002/slct.202100773>
37. Namkoong, J., Shin, S. S., Lee, H. J., Marín, Y. E., Wall, B. A., Goydos, J. S., & Chen, S. (2007). Metabotropic glutamate receptor 1 and glutamate signaling in human melanoma. *Cancer Research*, 67(5), 2298–2305. <https://doi.org/10.1158/0008-5472.can-06-3665>
38. Lewerenz, J., Hewett, S. J., Huang, Y., Lambros, M., Gout, P. W., Kalivas, P. W., Massie, A., Smolders, I., Methner, A., Pergande, M., Smith, S. B., Ganapathy, V., & Maher, P. (2013). The cystine/glutamate antiporter system x(c)(-) in health and disease: From molecular mechanisms to novel therapeutic opportunities. *Antioxidants and Redox Signaling*, 18(5), 522–555. <https://doi.org/10.1089/ars.2011.4391>
39. Zaharieva, E. K., Sasatani, M., & Kamiya, K. (2021). Kinetics of DNA repair under chronic irradiation at low and medium dose rates in repair proficient and repair compromised normal fibroblasts. *Radiation Research*, 197(4), 332–349.
40. Pittayapruek, P., Meeaphansan, J., Prapapan, O., Komine, M., & Ohtsuki, M. (2016). Role of matrix metalloproteinases in photoaging and photocarcinogenesis. *International Journal of Molecular Sciences*. <https://doi.org/10.3390/ijms17060868>
41. Shin, J. W., Kwon, S. H., Choi, J. Y., Na, J. I., Huh, C. H., Choi, H. R., & Park, K. C. (2019). Molecular mechanisms of dermal aging and antiaging approaches. *International Journal of Molecular Sciences*. <https://doi.org/10.3390/ijms20092126>
42. Buechner, N., Schroeder, P., Jakob, S., Kunze, K., Maresch, T., Calles, C., Krutmann, J., & Haendeler, J. (2008). Changes of MMP-1 and collagen type Ialpha1 by UVA, UVB and IRA are differentially regulated by Trx-1. *Experimental Gerontology*, 43(7), 633–637. <https://doi.org/10.1016/j.exger.2008.04.009>
43. Catalgol, B., Ziája, I., Breusing, N., Jung, T., Höhn, A., Alpertunga, B., Schroeder, P., Chondrogianni, N., Gonos, E. S., Petropoulos, I., Friguet, B., Klotz, L.-O., Krutmann, J., & Grune, T. (2009). The proteasome is an integral part of solar ultraviolet A radiation-induced gene expression*. *Journal of Biological Chemistry*, 284(44), 30076–30086. <https://doi.org/10.1074/jbc.M109.044503>
44. Jean, C., Bogdanowicz, P., Haure, M. J., Castex-Rizzi, N., Fournié, J. J., & Laurent, G. (2011). UVA-activated synthesis of metalloproteinases 1, 3 and 9 is prevented by a broad-spectrum sunscreen. *Photodermatology, Photoimmunology and Photomedicine*, 27(6), 318–324. <https://doi.org/10.1111/j.1600-0781.2011.00627.x>

Authors and Affiliations

I. Ivanova¹  · C. Bogner² · W. Gronwald² · M. Kreutz³ · B. Kurz¹ · T. Maisch¹ · Y. Kamenisch¹ · M. Berneburg¹

✉ I. Ivanova
Irina.Ivanova@ukr.de

✉ Y. Kamenisch
York.Kamenisch@ukr.de

✉ M. Berneburg
Mark.Berneburg@ukr.de

² Institute of Functional Genomics, University of Regensburg, Am BioPark 9, 93053 Regensburg, Germany

³ Department of Internal Medicine III, Molecular Oncology, University Hospital Regensburg, Franz-Josef-Strauss Allee 11, 93042 Regensburg, Germany

¹ Department of Dermatology, University Hospital Regensburg, 93042 Regensburg, Germany